MOLECULAR AND CELLULAR BIOLOGY, May 2006, p. 3707–3717 Vol. 26, No. 10
0270-7306/06/$08.00+0 doi:10.1128/MCB.26.10.3707–3717.2006

Mapping of DNA Replication Origins to Noncoding Genes of the X-Inactivation Center

Rebecca K. Rowntree and Jeannie T. Lee*

Howard Hughes Medical Institute, Department of Molecular Biology, Massachusetts General Hospital, Department of Genetics, Harvard Medical School, Boston, Massachusetts 02114

Received 27 February 2006/Returned for modification 28 February 2006/Accepted 3 March 2006

In mammals, few DNA replication origins have been identified. Although there appears to be an association between origins and epigenetic regulation, their underlying link to monoallelic gene expression remains unclear. Here, we identify novel origins of DNA replication (ORIs) within the X-inactivation center (*Xic*). We analyze 86 kb of the *Xic* using an unbiased approach and find an unexpectedly large number of functional ORIs. Although there has been a tight correlation between ORIs and CpG islands, we find that ORIs are not restricted to CpG islands and there is no dependence on transcriptional activity. Interestingly, these ORIs colocalize to important genetic elements or genes involved in X-chromosome inactivation. One prominent ORI maps to the imprinting center and to a domain within *Tsix* known to be required for X-chromosome counting and choice. Location and/or activity of ORIs appear to be modulated by removal of specific *Xic* elements. These data provide a foundation for testing potential relationships between DNA replication and epigenetic regulation in future studies.

DNA replication of mammalian chromosomes proceeds from a site or region known as the origin of bidirectional replication (ORI). There are estimated to be around 30,000 per genome with an average spacing of 100 kb (2). ORIs identified to date in *Saccharomyces cerevisiae* and bacteria are well-defined, specific sequences. In contrast, mammalian origins show no apparent sequence conservation other than an increased frequency of A/T nucleotides. Because of the high genome complexity and associated decrease in assay sensitivity, only a small number of mammalian ORIs have been identified to date.

Two extensively characterized ORIs illustrate the complexity and elusiveness of the ORI mechanism in mammals. Analysis of the ORI in the Chinese hamster dihydrofolate reductase gene (*DHFR*) has been aided by the fact that the Chinese hamster ovary cell line CHOC 400 contains a 1,000-fold amplification of this region (54) and therefore enables sensitive ORI detection. Several reports find that initiation can occur at discrete loci, as determined by leading strand direction analyses (12) and nascent strand abundance analyses (41). However, other studies which used two-dimensional gel electrophoresis analysis suggest that initiation sites are chosen from a large number of potential sites within a 55-kb initiation zone (26, 72). ORI characterization within the β-globin locus has also varied according to technique and species. In the murine locus, replication forks initiate from multiple locations within a broad zone of about 50 kb (4), but in humans, the locus instead uses a discrete ORI that is present between the two adult globin genes (40). These striking contrasts demonstrate the need for additional models in studying the nature and mechanism of DNA replication initiation in order to unify information gained using different experimental techniques.

* Corresponding author. Mailing address: Howard Hughes Medical Institute, Dept. of Molecular Biology, Massachusetts General Hospital, Boston, MA 02114. Phone: (617) 726-5943. Fax: (617) 726-6893. E-mail: lee@molbio.mgh.harvard.edu.

The collective data argue that the β-globin and *DHFR* ORIs can be influenced by multiple DNA elements at long range. Deletion of the β-globin locus control region, a region that controls the stage-specific expression of genes within the cluster, results in a switch in ORI usage (3). Deletion of the *DHFR* promoter, located at least 30 kb from the ORI region, reduces initiation from the *DHFR* ORI located 3′ of the gene, while introduction of a heterologous promoter restores initiation from the same ORI (63). These data clearly show a link between gene expression and ORI activity, thereby raising the question of whether ORIs may play a role in epigenetic regulation.

Indeed, recent studies reveal an interesting relationship between DNA replication and chromatin structure (53). Origin recognition complex (ORC) proteins and PCNA, an integral part of the replication fork complex, both affect gene expression and chromatin structure in the yeast mating type locus (73, 74). Moreover, histone H4 acetylation enhances the frequency of initiation in *Drosophila melanogaster* follicle cells (1). CpG islands, which are associated with gene promoters, are often enriched for ORI-containing sequences. Preparations of short nascent strand DNA that are enriched for ORIs are highly enriched for CpG islands (24). Further links between DNA replication and epigenetic phenomena are found in monoallelic gene regulation. For example, analyses of several imprinted murine genes show replication asynchrony between the maternally and paternally inherited alleles, with the paternal allele always replicating prior to the maternal allele even prior to the onset of monoallelic expression (39, 64). Genes in the odorant receptor clusters also show asynchronous replication (14, 65). In the immunoglobulin locus, the early-replicating κ allele almost always predetermines which allele will rearrange in B cells (56). However, it remains to be answered whether replication timing directly affects allelic choice and, if so, by what mechanism.

Here, we use X-chromosome inactivation (XCI) to interro-

TABLE 1. Sequences of primers used for real-time PCR analyses

Amplicon	Sequence (5′→3′)[a]
1	ACAAGGACTCCCTGCCTCAA
	CCCGGTTTCCACACTGATTT
2	GGGGGAGACAGACAGAGAGAGA
	ACTCACCCAGGGAATGATGG
3	TGGCTTCTTCTGGCTTCCAT
	CACAGTTGCGGCTCACTCTT
4	CCCCACCGAAATTCCTTTTT
	TTGCCACCTAGCCTCTGTGA
5	GGTATCTGGGAGCCCAACTG
	GGGGAAGGAAGGAGAATTGG
6	TGGCCTACTTGGCTTCACAA
	CTGGGAGGTTTTGCTCTTGG
7	CCTCCACTGCTCACATTCCA
	GGTGGTTGTCAACTGCCTG
8	TCAGCGATCCTGTCCAGATG
	GTGTTAGGCCCAGCCACTTC
9	TGGAGAGACTGGATGCCTGA
	GGGGAAGAGTTGGAGGAAGG
10	GCTGCCACCTGCTGGTTTAT
	GACGATCAAAGTGCCAGCAA
11	GCCACGGATACCTGTGTGTC
	CCGATGGGCTAAGGAGAAGA
12	AGCGCATGCTTGCAATTCTA
	TTGCACCGCCACGTATAGAG
13	AGCCCTGTGTGCATTTAGCA
	TGCAGAGGTTTTTGGCTGAA
14	TCCTGCAAGGGATACCGTTT
	AGAGCAGGTGGCAGTGCATA
15	TCCAACTGCTGGCACATTCT
	CAGTTGGCTCCTTCCTGGAG
16	ATCGCCATTATGCTGGGGTA
	TCTGGACCAACAAGGCAAAG
17	GCCATCTTTGGTCCCCATAA
	AGGCTCGAGCTACCACTGC
18	TCCCCACCATGTTATGACCA
	GCATTGTTTGGCTCAGTGCT
19	TGGCAAATATGCCCTGGAGT
	GAAACAGGGAAGGGCAAAGA
20	TCTTGAGCTGGCTGGACAGA
	CCAGAGTTCTGGGCCATAGG
21	TGAACATAACGGGGCTTGAA
	CCCAGTGCTGAACATGGGTA
22	ATTTGTGCAAGGCAGTGTGC
	ATCTCTGGCAGCAGCATTCA
23	CTGCAATGAGTGGGAAGCTG
	CTGCTGCAGCTCAAAAATGG
24	GGTACTGCAAGCGAGTGTGA
	CAGGAGGATCAGGAGCTCAG
25	ACGTGGAAGGCCAGATGCAC
	TGCAGCGACCCTAGCCATC
26	GCGGGAAGCCACCATGTTG
	AGCTTCACCTCACTGTGCC
27	ACAAACAAAGGGGCTGGAGA
	GCATTGGTGTTTTGCCTGAA
28	TGGCTACGGAGCAAACTCAA
	CACCACACCCTGCTCACAAT
29	ACACACACAAGCGCAAGAAAG
	GCTACCTGTGTCTCTGTATC
30	CTTGGTTACTTCACACGCTACC
	ACTACCTCACCGCACGTGTC
31	CGGGAACGTGGCATGTATGT
	AATGCCTGCGTAGTCCCGAA
32	AATGGCCCTTGGTGAGTGTT
	AGGTTTCCCTCAAACCCAGTCT
33	CCACAGTGTCCAATTTGTGC
	ATCGCCATTCCAAGCATAAG
34	TCCCCATATTCAAAGCTCTG
	TACCTACACCTACTTAGCAG
35	AGCTTGGCCTTCATGTGGAT
	CTCCCACCCTGACACATCAA
36	AACCGACGGGAAGGAAAACT
	GGGATCCCAGGTTGGAGAAT
37	GCCCTATGTGCAATCCCAAT
	TCATGGCATTTGTGAGCAGA
38	GGCCTTGTGAGCCTCTTGTA
	GATCTGCATCTCCTCCCTTG
39	TGCGCGTACATCACAAACAC
	TGAGCCTTGACACGTCGAAT
40	ATACAGGCACACGCACACAT
	CAGGGTCTTTTTGTCGTGGT
41	ACAGCCTCAACTAGCCTGGA
	CCTCGCATTTCCTGACACTT
42	GGCTGACCTCGAACTCACAA
	CTGGGGCTTATTTGGCGTAA
43	TTTGGTGGGTTTTTCGAGAC
	GGAGCTCTTGCCTTACATGG
44	TACCCACCGGAGCTAATGAC
	CACTCCAGAGGCAAAAGAGG
45	GGTGATTGTGAGCAGCTTGA
	GGAGGGGGAAAACAAGAAC
46	GGCTATCTACCCCCACCTTC
	GAGCTCTCCATCACCGTCTC
47	TTAATCCCACCAGCCCTCAG
	TAGCCCTGGGGAGCTAAGGT
48	CGGCAGCGCTAGAGAAAAAT
	AGGTGACACGCTTCAGCTTT
49	GCCCACTCCAGCACTAAAGG
	TGGGCAAGTATTGCACCTTG
50	CTTGGGGCTTTGCTTTTCAG
	CAATACCCGAGGCTCTCCAG
51	GGGGAGGTTGGGAGTCTAGG
	AGTACCGGACCCAACGAAGA
c-*Myc* A	CGGCATGATTTGGACGTAA
	AGCAACAGGCAAGGTATTCAACA
c-*Myc* B	AGCCCTGCCCCCATCCGACCT
	CTCTTTCCCCGCCCCCTCACC
c-*Myc* C	TTCTGTTTTCCCCAGCCTTA
	TCGGCTGAACTGTGTTCTTG
c-*Myc* D	TTTCTCACCTGTGCCCTAACCCT
	AGCCCGACTCCGACCTCT

[a] Top, forward; bottom, reverse.

gate potential relationships between DNA replication and epigenetic regulation in mammals. XCI equalizes X-chromosome gene dosage between the sexes in mammals by transcriptionally silencing one of two X's in the female (51). One of the earliest features of XCI is the asynchronous replication of the active (Xa) and inactive (Xi) X chromosomes (38), with the Xa chromosome replicating earlier in S phase than the Xi (68). DNA fluorescence in situ hybridization shows that replication asynchrony also occurs at the X-inactivation center (*Xic*) itself, although there is disagreement about whether the *Xist* allele on the Xa or that on the Xi replicates first (9, 33, 34, 70). One study observes that asynchrony is apparent even before the onset of XCI, but whether there is a preemptive role for DNA replication timing in determining allelic choice is not certain (33).

To investigate the link between DNA replication timing and epigenetic regulation at the *Xic*, we now seek to identify active

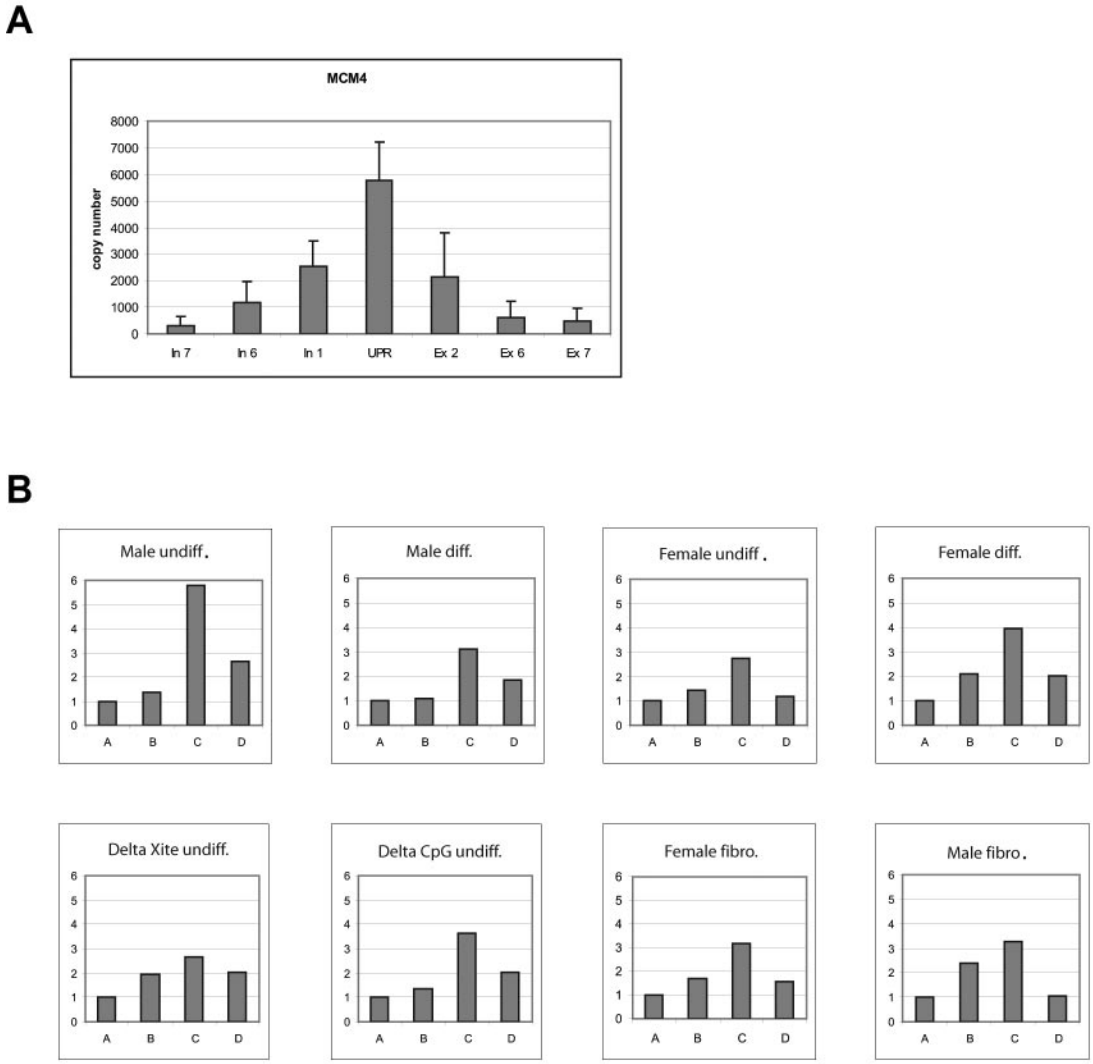

FIG. 1. Validation of the nascent strand analysis method. (A) Nascent strand abundance analysis of the *MCM4* locus in HeLa cells. Primer sequences and conditions are as previously described (43). Each bar gives the average of three experiments, and standard deviations are shown. In, intron; Ex, exon; UPR, upstream promoter region. (B) Graphs showing the ORIs at c-*Myc* locus for nascent strand preparations described in this work. Primer sequences and conditions are as previously described (31). diff., differentiated cells; undiff., undifferentiated cells; fibro., fibroblasts.

ORIs within the *Xic*, a regulatory region of at least 80 kb (48). At the *Xic*, three elements associated with noncoding transcripts have been identified so far. *Xist* initiates silencing and produces a noncoding transcript that "coats" the entire X chromosome (10, 11, 16, 60). *Xist* is regulated by its antisense partner, *Tsix* (46), which prevents up-regulation of Xist RNA in *cis* and designates the future Xa. Two putative ORIs have previously been associated with CpG islands at the 5′ promoter regions of *Xist* and *Tsix* (32). *Tsix* works in concert with the upstream *Xite* locus (58), which contains an enhancer and also promotes the persistence of *Tsix* on the future Xa (67). *Jpx*/*Enox* (15, 36) and the testes-specific gene *Tsx* (21) also reside at the *Xic*, but their functions have not been defined. Here, to determine the relationship between ORIs and known genetic elements of the *Xic*, we probe for ORI activity at 1.5-kb intervals across the entire 86-kb region and ask whether mutations of known *Xic* regulators affect origin usage.

MATERIALS AND METHODS

Cell lines and culture. Mouse embryonic stem (ES) cell lines J1 (40XY, 129Sv/J) (50) and EL16.7 (40XX, *Mus castaneus* × 129) (47) were maintained on gelatin-treated tissue culture flasks with a feeder layer of γ-irradiated mouse embryonic fibroblasts (obtained from day 13.5 [d13.5] embryos) in Dulbecco modified Eagle medium plus 15% fetal bovine serum (heat inactivated) and 500 U/ml leukemia inhibitory factor. Embryoid bodies were differentiated by use of suspension culture without leukemia inhibitory factor for 4 days and maintained thereafter under adherent conditions for 8 to 10 days. Primary fibroblasts were obtained from d13.5 embryos and maintained in Dulbecco modified Eagle medium plus 10% fetal bovine serum. The male deletion embryonic stem cell lines studied, $Xite^{\Delta L}$ (58) and $Tsix^{\Delta CpG}$ (47), were previously described.

Isolation of nascent strands. For nascent strand isolation, we followed the protocol of Kumar et al. (5, 25, 28, 35, 42, 43). Total genomic DNA was prepared from 1×10^8 exponentially growing cells. The use of asynchronously growing cells in the log phase of growth minimized the effects of cell cycle and replication timing in this assay. Cells were trypsinized and washed with cold phosphate-buffered saline and cold RBS (10 mM Tris-HCl [pH 7.4], 10 mM NaCl, 3 mM $MgCl_2$) before being resuspended in RBS at approximately 2.5×10^7 cells/ml and incubated on ice for 5 min. An equal volume of RBS containing 0.4% NP-40

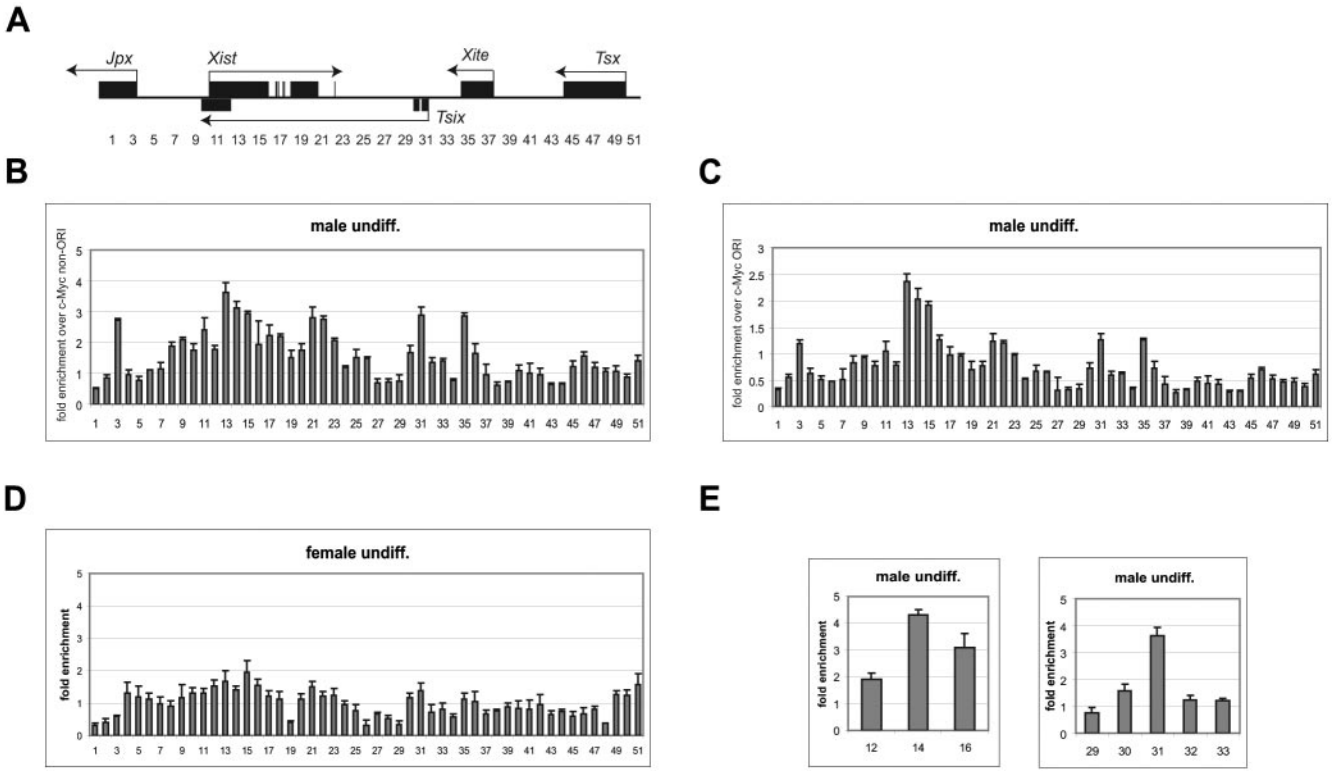

FIG. 2. Nascent strand abundance analysis of *Xic* region in wild-type ES cells. (A) Schematic of *Xic* region analyzed by real-time PCR. Genes are indicated by black rectangles and the direction of transcription is shown with an arrow. The locations of primer pairs studied are shown below. (B and C) Graphs of wild-type undifferentiated male ES cells normalized either to a murine c-*myc* non-ORI region encompassing the promoter (primer pair A) (shown in panel B) or to a c-*myc* ORI region (primer pair C) (shown in panel C) (31). Each bar shows the average of triplicate PCRs, and standard deviations are shown. (D) Graph of wild-type undifferentiated female ES cells normalized to the c-*myc* non-ORI region. (E) Average of three or four experiments at two ORI regions in male cells with standard errors shown.

was added, and the volumes were mixed and incubated on ice for 10 min. Nuclei were centrifuged at 850× *g* for 10 min at 4°C and washed with RBS before being resuspended at approximately 5×10^7 cells/ml. An equal volume of lysis buffer (20 mM Tris-HCl [pH 8], 20 mM EDTA [pH 8], 2% sodium dodecyl sulfate [SDS], 500 μg/ml proteinase K) was added and incubation took place at 50°C overnight. DNA was phenol:chloroform extracted and ethanol precipitated prior to resuspension at approximately 1 mg/ml.

Nascent strands were isolated by size fractionation on alkaline agarose gels as described previously (66). Briefly, 300 μg genomic DNA was denatured at 85°C for 10 min with 1/6 volume of 6× alkaline loading buffer (300 mM NaOH, 6 mM EDTA [pH 8], 18% Ficoll 400, 0.15% bromocresol green, 0.25% xylene cyanol) and rapidly chilled on ice for 10 min prior to electrophoresis on a 1.2% SeaPlaque (BMA) alkaline agarose gel containing 50 mM NaOH and 1 M EDTA, pH 8. Gel electrophoresis was carried out at 0.7 V/cm for 16 h at room temperature in 1× Tris-acetate-EDTA, 50 mM NaOH, 1 mM EDTA. The gel fragment containing DNA of 0.8 to 2 kb was excised and DNA was recovered using a QIAquick gel extraction kit (QIAGEN). Cell cycle synchronization, to enrich the population of cells in S phase, was not carried out, as ES cells spend the majority of their cell cycle in S phase (27). Bromodeoxyuridine labeling of the cells, to isolate only the replicating population, was also not performed, as previous studies have shown identical results with and without the use of bromodeoxyuridine affinity purification (42).

Nascent strand length analysis (NSLA). Size-fractionated nascent strands were isolated as described above. Fractions corresponding to 0.5 kb, 1.5 kb, 3 kb, 5 kb, and 12 kb were excised and purified using a QIAquick gel extraction kit (QIAGEN). An equal amount of DNA was added to PCR mixtures (equivalent to 2.5 ng of a 12-kb fraction). PCR was carried out for 30 cycles with an annealing temperature of 60°C. Appropriate control experiments were carried out to determine that these experiments were carried out under nonsaturating conditions. PCR products were purified using MultiScreen FB plates (Millipore) according to the manufacturer's instructions. Equal volumes of eluate were then transferred to Zeta probe membrane (Bio-Rad) by slot blotting according to the manufacturer's instructions. Membranes were probed with the cognate PCR products and exposed to phosphor screens overnight.

Real-time PCR analysis. PCR amplification was carried out with iQ SYBR green Supermix (Bio-Rad) using an iCycler iQ real-time detection system (Bio-Rad). The following conditions were used: 95°C for 8.5 min and 50 cycles of 95°C for 30 s, 60 to 65°C for 30 s, and 72°C for 30 s (primer sequences are shown in Table 1). Melt peak analysis was carried out for each reaction to confirm amplicon (amp.) specificity. Each reaction was performed in triplicate and repeated with at least two independent DNA preparations. The amount of nascent DNA in each independent preparation was calculated using a standard curve generated for every reaction with each primer pair, using four 10-fold dilutions of genomic DNA.

ChIP. Chromatin immunoprecipitation (ChIP) experiments were performed according to standard Abcam instructions. S7 micrococcal nuclease (1165 U; Roche) was added for 60 min at 4°C. Sonication was performed to produce DNA fragments of between 200 and 700 bp. Nuclei were centrifuged at 16,000 × *g* for 10 min at 4°C, and 100 μl of supernatant was diluted 10-fold with 900 μl ChIP dilution buffer (0.01% SDS, 1.1% Triton X-100, 1.2 mM EDTA, 16.7 mM Tris-HCl [pH 8.1], 167 mM NaCl plus protease inhibitors). The sonicate was precleared by incubation with 75 μl salmon sperm DNA-protein G or A-agarose slurry (Upstate) for 30 min at 4°C with agitation. Supernatant was collected and incubated with 50 μg ORC2 and ORC4 antibodies (sc-13238X and sc-20634X, respectively; Santa Cruz) at 4°C overnight with agitation. Thirty microliters of slurry was added and incubated, with agitation, at 4°C for 1 hour. The antibody/protein complexes were washed with 500 μl low-salt wash (0.1% SDS, 1% Triton X-100, 2 mM EDTA, 20 mM Tris-HCl [pH 8.1], 150 mM NaCl), high-salt wash (0.1% SDS, 1% Triton X-100, 2 mM EDTA, 20 mM Tris-HCl [pH 8.1], 500 mM NaCl), and lithium chloride wash (0.25 M LiCl, 1 mM EDTA, 10 mM Tris-HCl [pH 8.1], 1% deoxycholic acid) and then washed twice with TE (10 mM Tris-HCl [pH 8.1], 1 mM EDTA) prior to elution with 1% SDS-0.1 M $NaHCO_3$. Cross-links were reversed with the addition of 20 μl 5 M NaCl and 100 μg proteinase

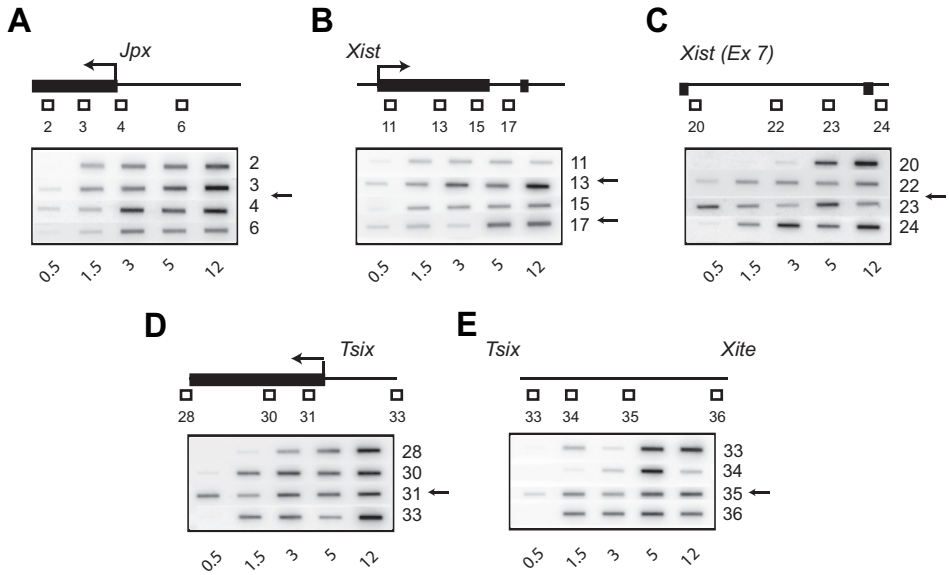

FIG. 3. Nascent strand length analysis confirms ORI locations. Each panel shows a schematic of the region analyzed. Exons are represented by black rectangles, and the directions of transcription are indicated by arrows. Primer locations are shown as open squares. The primer pair located closest to the ORI is indicated by an arrow. The sizes (kb) of the DNA fragments amplified are shown beneath each panel.

K at 65°C for 4 h prior to phenol:chloroform extraction and ethanol precipitation containing 20 μg glycogen carrier.

PCR was carried out using AmpliTaq Gold DNA polymerase (Applied Biosystems) for 34 cycles at 95°C for 30 s, 60°C for 30 s, and 72°C for 30 s. This was determined to be within the linear range of amplification for each primer pair tested. Each primer pair was tested on at least three independent chromatin samples. Quantitation was carried out using AlphaImager software (Alpha Innotech).

RESULTS

Identification of ORIs within the *Xic* by nascent strand abundance assay. Mammalian DNA replication proceeds bidirectionally from a point of origin and thus generates more copies of the DNA strands located closer to the origin than it does from those regions that are further away. Quantitative analysis of the relative amounts of DNA can therefore indicate the presence of a potential ORI. We first used the nascent strand abundance analysis (NSAA) technique (29). We generated single-stranded nascent DNA by size separation using alkaline gel electrophoresis and subsequent purification of the 0.8- to 2-kb fraction to enrich for short, ORI-containing strands while avoiding inclusion of short Okazaki fragments. To validate our technique, we first analyzed the *Mcm4* locus (43) in nascent strands obtained from HeLa cells and showed that we could detect the ORIs in these preparations (Fig. 1A). To determine the relative amounts of DNA across the *Xic*, we chose to do the assay in murine ES cells, an in vitro model in which the various steps of XCI can be examined during cell differentiation. We isolated nascent strands from wild-type undifferentiated ES cells as described above and tested for the presence of the previously reported ORI near the murine c-*Myc* promoter (31). Indeed, this ORI was detected in all nascent DNA samples generated (Fig. 1B and data not shown), indicating that our method was successful.

We then generated 51 pairs of primers at intervals of ~1.5 kb across the 86-kb *Xic* region spanning from *Jpx* to *Tsx* (Fig. 2A). Reaction conditions for each primer pair were extensively tested for real-time quantitative PCR (QPCR) to ensure that a single amplicon product without primer dimers was generated. QPCR was performed with ORI-enriched single-stranded nascent DNA for each primer set, and a standard curve was generated from a parallel preparation of genomic DNA for each amplicon. The relative copy number of DNA was determined at each amplicon position when normalized to the non-ORI region (primer pair A) from the murine c-*Myc* located on chromosome 15 (31) (Fig. 2B). Normalization to an ORI region of c-*Myc* (primer pair C) did not significantly alter the relative copy numbers for any of the analyses presented in this work (Fig. 2C and data not shown); thus, we arbitrarily chose to show only normalization to a non-ORI region in subsequent experiments.

In undifferentiated ES cells, five positions demonstrated an increase in nascent DNA abundance over the surrounding regions (Fig. 2B and D). These regions corresponded to the CpG island of *Jpx* (amp. 3 and 4), exon 1 (amp. 12 to 15) and intron 7 (amp. 21) within the *Xist* gene body, the CpG island of the *Tsix* promoter (amp. 31), and a region ~4 kb away from the *Xite* enhancer (amplicon 35). The highest peaks were five- to sixfold above background levels, consistent with enrichment observed at other ORIs (29, 32, 37, 69). (Of note is the fact that male peaks were consistently larger than female peaks in undifferentiated cultures. We believe that this reflected lower division rates of XX ES cells due to the toxicity of two active X's. Interestingly, the peak height differences between males and females disappear in embryoid body (EB) cultures, consistent with the occurrence of dosage compensation in female EBs [see Fig. 5]). The ORI spanning *Xist* exon 1 was broader than what is expected for a single ORI, a result that was especially apparent in females (Fig. 2D). This implies the presence of multiple active ORIs in this region. Two ORI regions (one corresponding to a CpG island and one not) were chosen

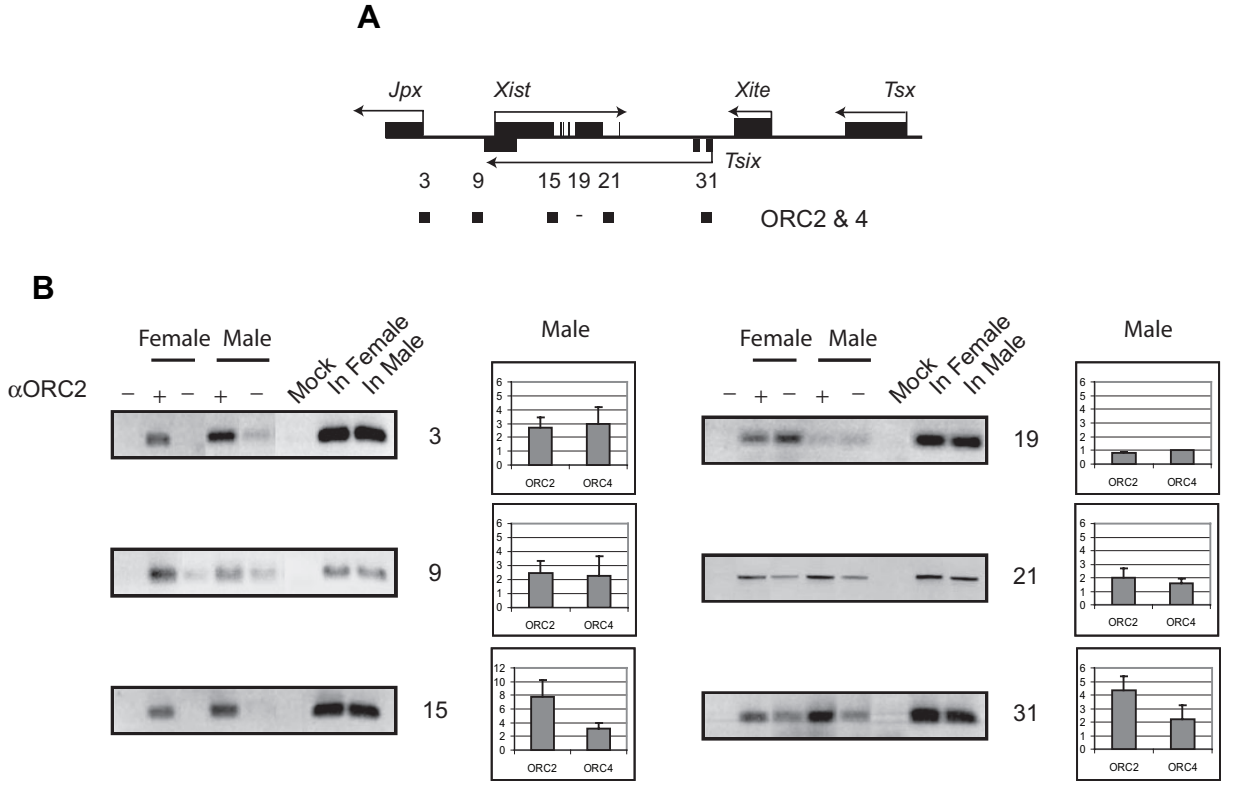

FIG. 4. Chromatin immunoprecipitation shows ORC binding at ORI regions. (A) Schematic diagram of *Xic* region. Locations of primer pairs used for ChIP assay and a summary of the ORC binding are indicated below. (B) Left lane of each panel shows the negative PCR control. α-ORC2 antibodies were added as indicated above to formaldehyde cross-linked female (EL16.7) and male (J1) undifferentiated ES cells. "Mock" denotes the control (no cells); 1:100 dilutions of starting material were used for input lanes. One representative ChIP is shown for each primer pair. Histograms show the average ORC2 or ORC4 enrichment over that of minus-antibody controls in three to six independent experiments with male cells with standard deviations shown. Similar results were gained with female cells (data not shown).

for further analysis by NSAA. In three or four independent cell preparations, both regions were found to be enriched in the nascent strand pool (Fig. 2E), further indicating the presence of origin activity at these positions. Cumulatively, these findings revealed putative ORI activity at five locations within the *Xic*.

Confirmation of ORIs using nascent strand length analysis and chromatin immunoprecipitation assays. The density of the putative ORI identified above is unusual for a mammalian genome. To confirm the results of NSAA, we carried out NSLA (71) and chromatin immunoprecipitations for ORI-associated proteins. By use of NSLA, we isolated single-stranded DNA fragments of increasing size from asynchronously growing cells as described for the NSAA above. We then carried out PCR using primers surrounding the ORI regions and quantified the PCR products by probing with the cognate PCR fragment. In theory, the ORI regions would be present in the shortest fragments of nascent DNA isolated, whereas regions further from the ORIs would be present only in longer nascent fragments that have extended away from the ORIs.

Using NSLA, we found that sequences containing the ORI located at the *Tsix* gene promoter were present in the shortest fragments of DNA tested (<1 kb) (Fig. 3D), consistent with the findings of Gomez and Brockdorff (32). Interestingly, this method suggested that the broad activity zone detected by NSAA at the 5′ end *Xist* exon 1 may actually reflect the activity of two distinct ORIs at positions 13 and 17 (Fig. 3B). In addition, we detected ORI activity at the *Jpx* CpG island, the *Xist* exon 1 region, and *Xist* intron 7 and near *Xite* (Fig. 3), as indicated above, by NSAA. Thus, the nascent strand abundance and length assays yielded essentially identical results.

We then utilized ChIP as a third and independent approach to verifying ORI activity. The ChIP assay is based on the association of ORIs with specific regulatory proteins. Current dogma dictates that DNA replication is initiated by the binding of "initiator" proteins called ORC to the ORI (7). To determine whether the putative *Xic* ORI bound such proteins, we performed ChIP using antibodies against ORC2, a regulator detected at all ORIs investigated to date (8). In both male and female undifferentiated ES cells, we found ORC2 binding in vivo at the putative ORI sites 3, 15, 21, and 31, as shown by an enrichment of the amplicon produced over that produced by minus-antibody control reactions (Fig. 4B). In contrast, no enrichment of ORC2 antibody-derived chromatin was detected over the minus-antibody controls at region 19, located between ORI regions. Since ORC proteins have many cellular functions, we also tested the localization of ORC4, and results similar to those for ORC2 were generated at all amplicons tested (Fig. 4B). The region just upstream of the *Xist* promoter (amp. 9) had previously been identified as an ORI (32). Al-

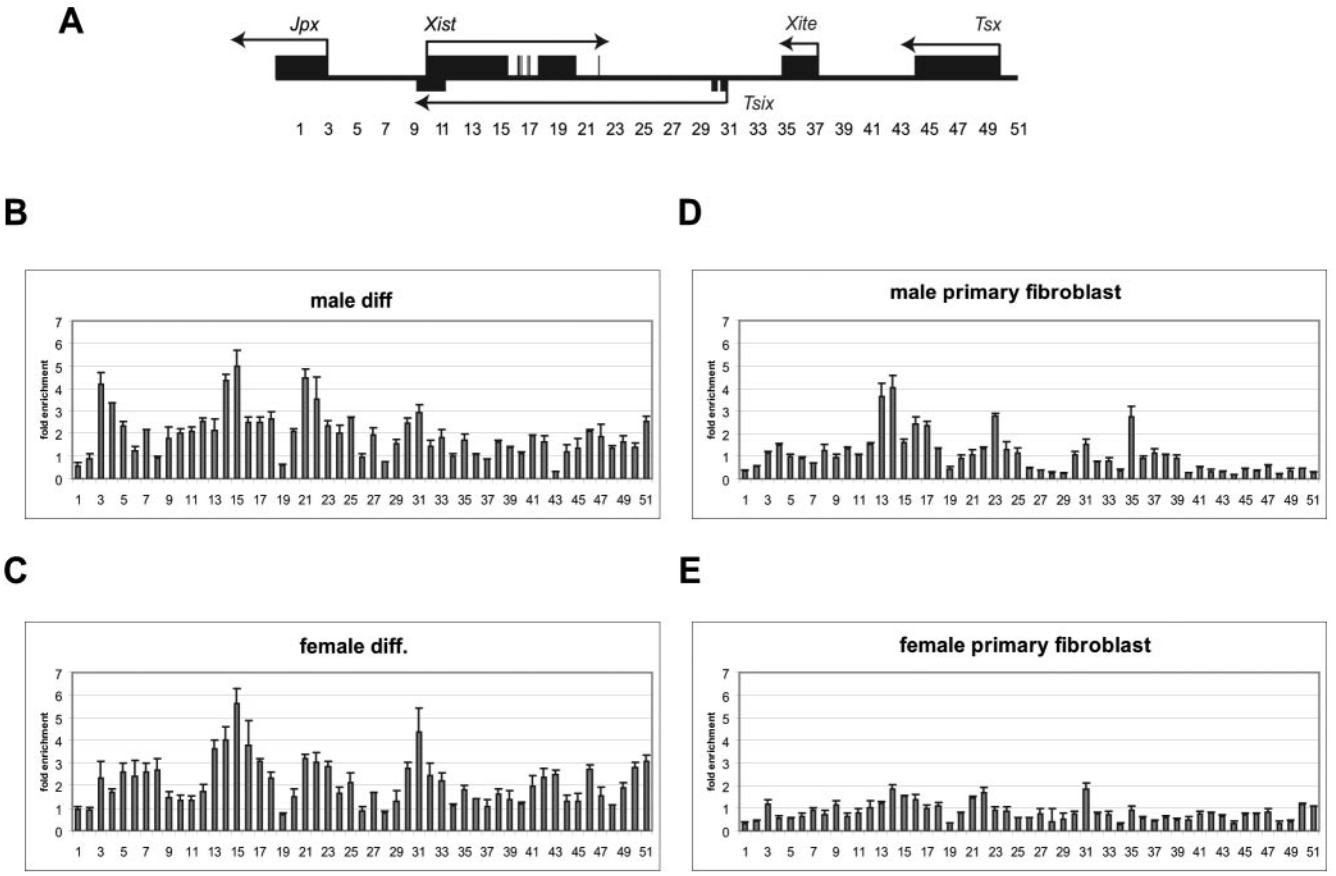

FIG. 5. Nascent strand abundance analysis of the *Xic* region in differentiated cell types. (A) Schematic of *Xic* region analyzed by real-time PCR. Genes are indicated by black rectangles, and the directions of transcription are shown with arrows. The locations of primer pairs studied are shown below. Real-time PCR analysis as described in the legend for Fig. 1 of (B) male J1 and (C) female EL16.7 differentiated (d12) ES cells, (D) male primary fibroblasts, and (E) female primary fibroblasts is shown. All graphs indicate enrichment over c-*Myc* non-ORI (primer pair A).

though our NSAA found only a modest increase in abundance at this position, the ORC ChIP assay did show slight enrichment for ORC2 and ORC4 (Fig. 4B) at amplicon 9. Taken together, these experiments confirmed the existence of multiple ORI activities at the *Xic* in ES cells.

Dynamic changes in origin usage during cell differentiation and XCI. To assess the relationship between ORIs and events of XCI, we next addressed the question of whether ORI usage changes when cells proceed down the XCI pathway. We induced ES cell differentiation and observed no significant changes in ORI positioning from that for undifferentiated preinactivation cells (Fig. 5B and C). This result indicated that the same origins were used in pre- and postinactivation cells. Consistent ORI usage has been observed at other X-linked ORIs. For example, the intron 1 ORI of *HPRT*/*Hprt* (17, 19) and the CpG island-associated ORI of *G6PD* (18) are used regardless of X-chromosome activity (Xa versus Xi). The murine β-globin also demonstrates no significant shifts in ORI usage in various physiological states (4).

However, while ORI positions were conserved upon cell differentiation, their degree of usage may vary slightly, as intensities of individual peaks did change. For example, the *Jpx* ORI (amp. 3) appeared to intensify during differentiation, while the *Xite* ORI (amp. 35) appeared to diminish in activity (Fig. 5B and C). The same QPCR analysis was then performed using primary fibroblasts, a somatic cell type in which XCI has already occurred. Similar peaks suggestive of ORIs could be observed in both male and female fibroblasts (Fig. 5D and E), although there was a trend towards less ORI activity in both fibroblast lines that was perhaps in keeping with their lower mitotic rates. Cumulatively, these results demonstrated that the five *Xic* ORIs are used, to differing degrees, at all stages during development.

***Xic* mutations affect ORI position and activity.** To determine whether changes in ORI function occur in the presence of specific *Xic* mutations, we investigated ORI activity in cells with deletions of *Tsix* and *Xite*, two regulators of XCI initiation. In each case, we isolated the mutant X in a male background so as to restrict analyses specifically to the affected X. Because male ES cells are capable of up-regulating *Xist* and undergoing XCI when carrying *Xic* transgenes, they contain all necessary *trans* factors involved in XCI (49).

We first examined the effects of deleting *Xite*, a locus that determines X-chromosome counting choice by acting synergistically in *cis* with *Tsix*. The $Xite^{\Delta L}$ allele skews the ratio of XCI in favor of silencing the mutated X in the XX female (58) and contains a 12-kb deletion that includes the *Xite* enhancer (67), transcription start sites of the noncoding *Xite* transcripts, and a

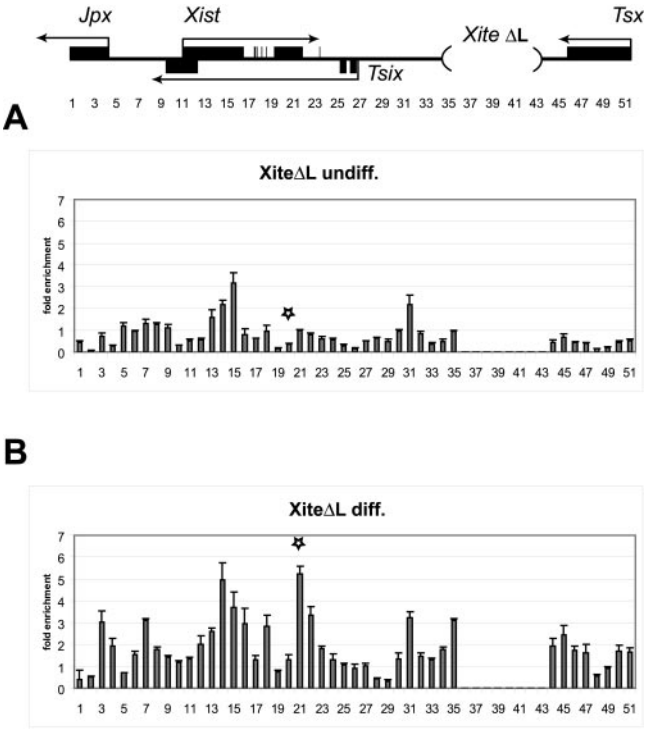

FIG. 6. Removal of genetic elements important for XCI alters ORI activity. A map showing the *Xic* region and the corresponding genomic deletion is shown above. Real-time PCR analysis as described in the legend for Fig. 1 of (A) $Xite^{\Delta L}$ undifferentiated (d0) male ES cells and (B) $Xite^{\Delta L}$ differentiated (d12) ES cells is shown. All graphs indicate enrichment over c-*Myc* non-ORI (primer pair A). Black stars indicate the most different ORI peak, as discussed in the text.

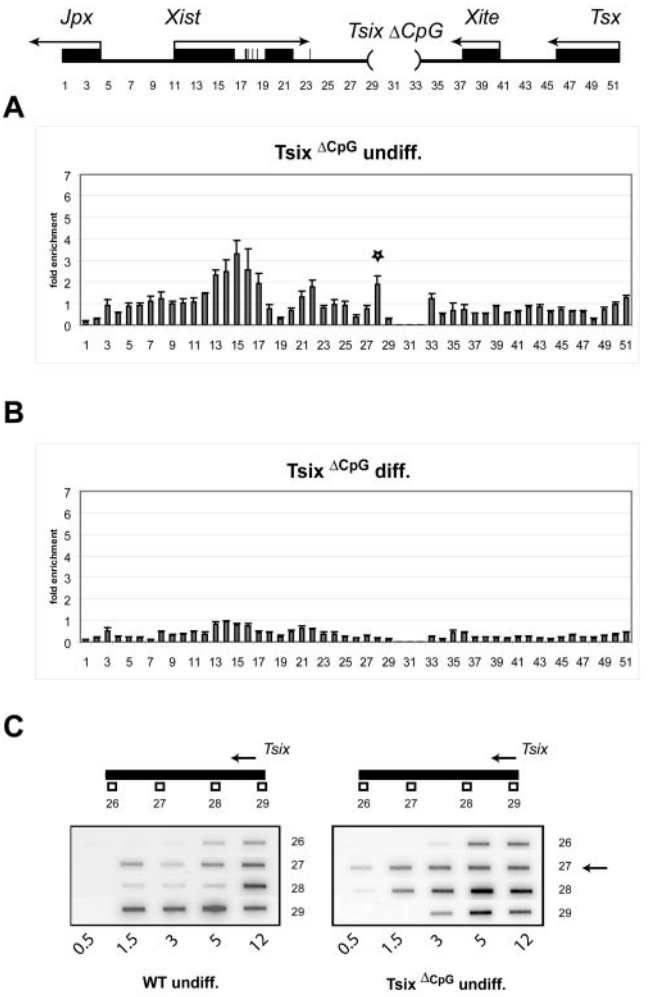

FIG. 7. Removal of CpG island and *Tsix* promoter alters ORI activity. A map showing the *Xic* region and the corresponding genomic deletion is shown above. Real-time PCR analysis as described in the legend for Fig. 1 of (A) $Tsix^{\Delta CpG}$ undifferentiated (d0) male ES cells and (B) $Tsix^{\Delta CpG}$ differentiated (d12) ES cells is shown. All graphs indicate enrichment over c-*Myc* non-ORI (primer pair A). (C) Nascent strand length analysis as described in the legend for Fig. 3 in wild-type (WT) and deleted male undifferentiated cells.

minor ORI (amp. 35 to 37). Nascent strand analysis by QPCR revealed that the $Xite^{\Delta L}$ line exhibited significant differences from wild-type male ES cells. In undifferentiated cells, the removal of this element resulted in markedly reduced activity of all the ORIs compared to that for wild-type cells (Fig. 6A). This decrease was most evident for the ORI at amplicon 21, which was greatly reduced even in comparison to the rest of the *Xic* in this cell line. However, the ORI located at the *Xist* promoter region (Fig. 2 and 3 and reference 32) becomes more apparent. Thus, deletion of the choice determinant, *Xite*, and of its associated minor ORI modulated the activity and position of other ORIs at a considerable distance across the *Xic*.

We next examined the effect of deleting *Tsix*, the antisense partner of *Xist* that prevents the up-regulation of the silencing Xist RNA on the future Xa chromosome. The $Tsix^{\Delta CpG}$ line (47) carries a 3.7-kb deletion including the *Tsix* promoter, the associated *DXPas34* repeat element (20, 23), various enhancer elements (20, 23, 67), and the *Tsix* promoter ORI identified above (amp. 31). The $Tsix^{\Delta CpG}$ mutation also had significant effects on the presence or activity of the remaining ORIs. Although the activity of the ORI located at amplicon 21 appeared to be similar to that of the wild-type undifferentiated male cells, the abundances of amplicons 3 and 35 were significantly reduced (Fig. 7A). Additionally, a new peak arose at amplicon 28, where no ORI had previously been observed; this suggested that deletion of the *Tsix* ORI permitted the use of a nearby ORI. The presence of this ORI was confirmed using NSLA (Fig. 7C). A clear difference was observed between the mutant cells, where short, nascent DNA fragments were present at amplicons 27 and 28, and the wild-type cells, from which these fragments were absent. While the positions of the ORIs remained unchanged upon cellular differentiation, a drastic reduction in activity at all the ORI regions was observed (Fig. 7B). Taken together, the results with $Xite^{\Delta L}$ and $Tsix^{\Delta CpG}$ suggest that ORI usage at the *Xic* can be modulated by mutations in *Xite* and *Tsix*. Disrupting these loci results in a shift both in ORI position and in the frequency of usage of different ORIs.

DISCUSSION

Mammalian ORIs have become a main interest of epigenetic studies (4, 22), but few ORIs have been characterized in detail. In general, it is thought that eukaryotic genomes repli-

cate using many hundreds of replication ORIs spaced at 50- to 300-kb intervals, but the actual density of ORIs has not been addressed systematically, since many studies have concentrated on discrete CpG islands and single genes (30). Using a real-time QPCR approach, we have now analyzed 86 kb of an X-linked region with five transcribed units and found at least five ORIs. These ORIs were defined independently by NSAA, NSLA, and ChIP. It has been suggested that most if not all CpG islands may have ORI activity (6). Our data are consistent with this idea, as all of the CpG islands now analyzed within the *Xic* can function as ORIs (this work and reference 32). However, not all ORIs are associated with CpG islands. At the *Xic*, ORI activity could also be detected within *Xist* exon 1 and intron 7.

These results speak directly to the hypothesis that transcription may be required for origin activity. The necessity of transcription has been suggested by the coincidence of many ORIs with CpG islands (6) and by the finding that active transcription through the *DHFR* gene increases the efficiency of firing from the ORI located 3′ to the gene, while a deletion compromises it (63). An open chromatin conformation that enables transcription factor binding may simultaneously allow ORC proteins to bind, consistent with the observation that active transcription is often associated with early replication. As shown here and elsewhere (32), however, a requirement for active transcription does not occur at *Xic* ORIs. The most prominent ORI identified in this study occurs within exon 1 of *Xist*. This ORI apparently fires regardless of the transcriptional activity of the *Xist* gene, as it is detected both in undifferentiated ES cells and in somatic XY cells where *Xist* is off. Likewise, the ORI within intron 7 of *Xist* can fire in the same *Xist*-off cells.

As observed here, an average ORI spacing of one per 15 kb is much higher than what is predicted by genome averages. However, a recent, elegant study of the IgH locus also identified origins spaced every 20 kb throughout a 300-kb region (57). In addition to the five constitutive ORIs at the *Xic*, we have also found at least one cryptic ORI whose activity is uncovered only when a nearby ORI is deleted. With six potential ORIs to choose from, the usage within any one cell may vary from using all to using only a small subset of the ORIs. The use of standard population-based assays precludes distinction between these possibilities. Studies with the IgH locus suggest that a small number of possible origins are used on each allele during a single duplication cycle (57).

Our results are largely consistent with those of Gomez and Brockdorff, who used NSLA and NSAA to identify two ORIs coinciding with the CpG islands of *Xist* and *Tsix* (32). However, several differences with regard to the pattern of usage should be discussed. First, while those authors reported prominent usage of the ORIs at the *Xist* promoter, we find that ORIs within internal regions of *Xist* have more intense activity. Second, the ORI usage at the *Tsix* promoter was reported by Gomez and Brockdorff to be XX dependent, as XY cells show minimal activity. However, we consistently observe ORI activity at the *Tsix* promoter in both XX and XY cells, both undifferentiated and differentiated. Finally, our data demonstrate the presence of many other ORIs at the *Xic*, with the activities of some ORIs clearly mutable by differentiation state and by the deletion of critical XCI regulators. These differences could have resulted from different methodologies or different cell lines used.

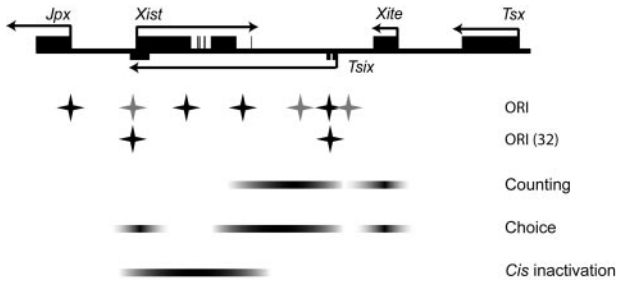

FIG. 8. ORIs at the *Xic*. A schematic of the *Xic* region is shown. Locations of active ORIs are denoted as black stars, with less active ORIs shown as gray stars. The genetic elements involved in XCI are shown beneath.

It is interesting that ORIs coincide with regulatory noncoding elements (Fig. 8). *Xist* has been shown to control both X-chromosome choice (52, 61) and the initiation of chromosome-wide silencing (60). In fact, one of the regions implicated in choice (52) roughly coincides with the exonic ORI mapped to amplicons 14 to 16. At the 5′ end of *Tsix*, an ORI (amp. 31) maps to the prominent CpG island near the transcription start site, a region of considerable interest in terms of how *Xist* is blocked from initiating silencing on the future Xa chromosome. This 5′ domain of *Tsix* has been shown to contain an imprinting center that regulates paternal allele-specific silencing of the X in placental tissues (44, 62). It also harbors elements required for X-chromosome counting and stochastic allelic choice (45, 47, 55) and includes the repeat element *DXPas34* (23), a *Tsix*-specific bipartite enhancer (67), and binding sites for the chromatin insulator CTCF (13). In *Xite*, the minor ORI (amp. 35 to 37) localizes near the second of two CpG islands and transcription start sites in this locus. This domain of *Xite* has also been implicated in X-chromosome choice (47) and counting (45, 55). The ORI at amplicon 3 lies in the CpG island of *Jpx/Enox*, a gene of unknown function that is expressed at least partially from both Xa and Xi. Because *Jpx/Enox* is located within a 30-kb interval upstream of *Xist* that has been shown by genetic analysis to be required for *Xist* regulation (48), this noncoding RNA may also play a significant role in XCI.

The mapping of ORIs to elements that regulate XCI (Fig. 8) raises the possibility that epigenetic regulation and DNA replication may be physiologically linked. Indeed, we have shown that deleting critical domains of *Xite* and *Tsix* can modulate both the frequency of specific ORI usage and the recruitment of previously underused ORIs to the task. After removal of the *Tsix* promoter ($Tsix^{\Delta CpG}$), we observe an alteration in ORI location and intensity more than 6 kb away. These data are similar to those of Paixao et al., who show that the removal of a nearby CpG island from the human *laminB2* ORI results in a reduction of activity of the related ORI (59). When *Xite* is deleted ($Xite^{\Delta L}$), we observe a long-range effect more than 30 kb away (position 21). Future work will address whether these ORI modulations in turn regulate the events of XCI. It is relevant that differential replication timing of the *Xic* has been noted previously (9, 34, 70) and is one potential mechanism by

which allelic choice might be regulated. Our findings pave the way for investigation into whether and how DNA replication influences epigenetic structure and the pattern of asymmetric gene expression during development.

ACKNOWLEDGMENTS

We thank Khanh Huynh, Montserrat Anguera, Bryan Sun, and Steve Bell for helpful comments on the manuscript.

This work was supported by NIH grant R01 (GM38895) and the MGH Fund for Medical Discovery Postdoctoral Fellowship (R.K.R.). J.T.L. is an Investigator of the Howard Hughes Medical Institute.

REFERENCES

1. **Aggarwal, B. D., and B. R. Calvi.** 2004. Chromatin regulates origin activity in Drosophila follicle cells. Nature **430:**372–376.
2. **Aladjem, M. I., and E. Fanning.** 2004. The replicon revisited: an old model learns new tricks in metazoan chromosomes. EMBO Rep. **5:**686–691.
3. **Aladjem, M. I., M. Groudine, L. L. Brody, E. S. Dieken, R. E. Fournier, G. M. Wahl, and E. M. Epner.** 1995. Participation of the human beta-globin locus control region in initiation of DNA replication. Science **270:**815–819.
4. **Aladjem, M. I., L. W. Rodewald, C. M. Lin, S. Bowman, D. M. Cimbora, L. L. Brody, E. M. Epner, M. Groudine, and G. M. Wahl.** 2002. Replication initiation patterns in the β-globin loci of totipotent and differentiated murine cells: evidence for multiple initiation regions. Mol. Cell. Biol. **22:**442–452.
5. **Altman, A. L., and E. Fanning.** 2001. The Chinese hamster dihydrofolate reductase replication origin beta is active at multiple ectopic chromosomal locations and requires specific DNA sequence elements for activity. Mol. Cell. Biol. **21:**1098–1110.
6. **Antequera, F., and A. Bird.** 1999. CpG islands as genomic footprints of promoters that are associated with replication origins. Curr. Biol. **9:**R661–R667.
7. **Bell, S. P., and B. Stillman.** 1992. ATP-dependent recognition of eukaryotic origins of DNA replication by a multiprotein complex. Nature **357:**128–134.
8. **Bielinsky, A. K., and S. A. Gerbi.** 2001. Where it all starts: eukaryotic origins of DNA replication. J. Cell Sci. **114:**643–651.
9. **Boggs, B. A., and A. C. Chinault.** 1997. Analysis of DNA replication by fluorescence in situ hybridization. Methods **13:**259–270.
10. **Brockdorff, N., A. Ashworth, G. F. Kay, V. M. McCabe, D. P. Norris, P. J. Cooper, S. Swift, and S. Rastan.** 1992. The product of the mouse Xist gene is a 15 kb inactive X-specific transcript containing no conserved ORF and located in the nucleus. Cell **71:**515–526.
11. **Brown, C. J., B. D. Hendrich, J. L. Rupert, R. G. Lafreniere, Y. Xing, J. Lawrence, and H. F. Willard.** 1992. The human XIST gene: analysis of a 17 kb inactive X-specific RNA that contains conserved repeats and is highly localized within the nucleus. Cell **71:**527–542.
12. **Burhans, W. C., L. T. Vassilev, M. S. Caddle, N. H. Heintz, and M. L. DePamphilis.** 1990. Identification of an origin of bidirectional DNA replication in mammalian chromosomes. Cell **62:**955–965.
13. **Chao, W., K. D. Huynh, R. J. Spencer, L. S. Davidow, and J. T. Lee.** 2002. CTCF, a candidate trans-acting factor for X-inactivation choice. Science **295:**345–347.
14. **Chess, A., I. Simon, H. Cedar, and R. Axel.** 1994. Allelic inactivation regulates olfactory receptor gene expression. Cell **78:**823–834.
15. **Chureau, C., M. Prissette, A. Bourdet, V. Barbe, L. Cattolico, L. Jones, A. Eggen, P. Avner, and L. Duret.** 2002. Comparative sequence analysis of the X-inactivation center region in mouse, human, and bovine. Genome Res. **12:**894–908.
16. **Clemson, C. M., J. A. McNeil, H. F. Willard, and J. B. Lawrence.** 1996. XIST RNA paints the inactive X chromosome at interphase: evidence for a novel RNA involved in nuclear/chromosome structure. J. Cell Biol. **132:**259–275.
17. **Cohen, S. M., B. P. Brylawski, M. Cordeiro-Stone, and D. G. Kaufman.** 2002. Mapping of an origin of DNA replication near the transcriptional promoter of the human HPRT gene. J. Cell. Biochem. **85:**346–356.
18. **Cohen, S. M., B. P. Brylawski, M. Cordeiro-Stone, and D. G. Kaufman.** 2003. Same origins of DNA replication function on the active and inactive human X chromosomes. J. Cell. Biochem. **88:**923–931.
19. **Cohen, S. M., S. Hatada, B. P. Brylawski, O. Smithies, D. G. Kaufman, and M. Cordeiro-Stone.** 2004. Complementation of replication origin function in mouse embryonic stem cells by human DNA sequences. Genomics **84:**475–484.
20. **Courtier, B., E. Heard, and P. Avner.** 1995. Xce haplotypes show modified methylation in a region of the active X chromosome lying 3′ to Xist. Proc. Natl. Acad. Sci. USA **92:**3531–3535.
21. **Cunningham, D. B., D. Segretain, D. Arnaud, U. C. Rogner, and P. Avner.** 1998. The mouse Tsx gene is expressed in Sertoli cells of the adult testis and transiently in premeiotic germ cells during puberty. Dev. Biol. **204:**345–360.
22. **Danis, E., K. Brodolin, S. Menut, D. Maiorano, C. Girard-Reydet, and M. Mechali.** 2004. Specification of a DNA replication origin by a transcription complex. Nat. Cell Biol. **6:**721–730.
23. **Debrand, E., C. Chureau, D. Arnaud, P. Avner, and E. Heard.** 1999. Functional analysis of the *DXPas34* locus, a 3′ regulator of *Xist* expression. Mol. Cell. Biol. **19:**8513–8525.
24. **Delgado, S., M. Gomez, A. Bird, and F. Antequera.** 1998. Initiation of DNA replication at CpG islands in mammalian chromosomes. EMBO J. **17:**2426–2435.
25. **Dijkwel, P. A., and J. L. Hamlin.** 1999. Physical and genetic mapping of mammalian replication origins. Methods **18:**418–431.
26. **Dijkwel, P. A., S. Wang, and J. L. Hamlin.** 2002. Initiation sites are distributed at frequent intervals in the Chinese hamster dihydrofolate reductase origin of replication but are used with very different efficiencies. Mol. Cell. Biol. **22:**3053–3065.
27. **Fujii-Yamamoto, H., J. M. Kim, K. Arai, and H. Masai.** 2005. Cell cycle and developmental regulations of replication factors in mouse embryonic stem cells. J. Biol. Chem. **280:**12976–12987.
28. **Giacca, M., C. Pelizon, and A. Falaschi.** 1997. Mapping replication origins by quantifying relative abundance of nascent DNA strands using competitive polymerase chain reaction. Methods **13:**301–312.
29. **Giacca, M., L. Zentilin, P. Norio, S. Diviacco, D. Dimitrova, G. Contreas, G. Biamonti, G. Perini, F. Weighardt, S. Riva, et al.** 1994. Fine mapping of a replication origin of human DNA. Proc. Natl. Acad. Sci. USA **91:**7119–7123.
30. **Gilbert, D. M.** 2004. In search of the holy replicator. Nat. Rev. Mol. Cell Biol. **5:**848–855.
31. **Girard-Reydet, C., D. Gregoire, Y. Vassetzky, and M. Mechali.** 2004. DNA replication initiates at domains overlapping with nuclear matrix attachment regions in the xenopus and mouse c-myc promoter. Gene **332:**129–138.
32. **Gomez, M., and N. Brockdorff.** 2004. Heterochromatin on the inactive X chromosome delays replication timing without affecting origin usage. Proc. Natl. Acad. Sci. USA **101:**6923–6928.
33. **Gribnau, J., S. Luikenhuis, K. Hochedlinger, K. Monkhorst, and R. Jaenisch.** 2005. X chromosome choice occurs independently of asynchronous replication timing. J. Cell Biol. **168:**365–373.
34. **Hansen, R. S., T. K. Canfield, and S. M. Gartler.** 1995. Reverse replication timing for the XIST gene in human fibroblasts. Hum. Mol. Genet. **4:**813–820.
35. **Hu, L., X. Xu, and M. S. Valenzuela.** 2004. Initiation sites for human DNA replication at a putative ribulose-5-phosphate 3-epimerase gene. Biochem. Biophys. Res. Commun. **320:**648–655.
36. **Johnston, C., A. Newall, N. Brockdorff, and T. Nesterova.** 2002. Enox, a novel gene that maps 10 kb upstream of Xist and partially escapes X inactivation. Genomics **80:**236.
37. **Keller, C., E. M. Ladenburger, M. Kremer, and R. Knippers.** 2002. The origin recognition complex marks a replication origin in the human TOP1 gene promoter. J. Biol. Chem. **277:**31430–31440.
38. **Keohane, A. M., L. P. O'Neill, N. D. Belyaev, J. S. Lavender, and B. M. Turner.** 1996. X-Inactivation and histone H4 acetylation in embryonic stem cells. Dev. Biol. **180:**618–630.
39. **Kitsberg, D., S. Selig, M. Brandeis, I. Simon, I. Keshet, D. J. Driscoll, R. D. Nicholls, and H. Cedar.** 1993. Allele-specific replication timing of imprinted gene regions. Nature **364:**459–463.
40. **Kitsberg, D., S. Selig, I. Keshet, and H. Cedar.** 1993. Replication structure of the human beta-globin gene domain. Nature **366:**588–590.
41. **Kobayashi, T., T. Rein, and M. L. DePamphilis.** 1998. Identification of primary initiation sites for DNA replication in the hamster dihydrofolate reductase gene initiation zone. Mol. Cell. Biol. **18:**3266–3277.
42. **Kumar, S., M. Giacca, P. Norio, G. Biamonti, S. Riva, and A. Falaschi.** 1996. Utilization of the same DNA replication origin by human cells of different derivation. Nucleic Acids Res. **24:**3289–3294.
43. **Ladenburger, E. M., C. Keller, and R. Knippers.** 2002. Identification of a binding region for human origin recognition complex proteins 1 and 2 that coincides with an origin of DNA replication. Mol. Cell. Biol. **22:**1036–1048.
44. **Lee, J. T.** 2000. Disruption of imprinted X inactivation by parent-of-origin effects at Tsix. Cell **103:**17–27.
45. **Lee, J. T.** 2005. Regulation of X-chromosome counting by Tsix and Xite sequences. Science **309:**768–771.
46. **Lee, J. T., L. S. Davidow, and D. Warshawsky.** 1999. Tsix, a gene antisense to Xist at the X-inactivation centre. Nat. Genet. **21:**400–404.
47. **Lee, J. T., and N. Lu.** 1999. Targeted mutagenesis of Tsix leads to nonrandom X inactivation. Cell **99:**47–57.
48. **Lee, J. T., N. Lu, and Y. Han.** 1999. Genetic analysis of the mouse X inactivation center defines an 80-kb multifunction domain. Proc. Natl. Acad. Sci. USA **96:**3836–3841.
49. **Lee, J. T., W. M. Strauss, J. A. Dausman, and R. Jaenisch.** 1996. A 450 kb transgene displays properties of the mammalian X-inactivation center. Cell **86:**83–94.
50. **Li, E., T. H. Bestor, and R. Jaenisch.** 1992. Targeted mutation of the DNA methyltransferase gene results in embryonic lethality. Cell **69:**915–926.
51. **Lyon, M. F.** 1961. Gene action in the X-chromosome of the mouse (Mus musculus L.). Nature **190:**372–373.
52. **Marahrens, Y., J. Loring, and R. Jaenisch.** 1998. Role of the Xist gene in X chromosome choosing. Cell **92:**657–664.
53. **McNairn, A. J., and D. M. Gilbert.** 2003. Epigenomic replication: linking epigenetics to DNA replication. Bioessays **25:**647–656.

54. **Milbrandt, J. D., N. H. Heintz, W. C. White, S. M. Rothman, and J. L. Hamlin.** 1981. Methotrexate-resistant Chinese hamster ovary cells have amplified a 135-kilobase-pair region that includes the dihydrofolate reductase gene. Proc. Natl. Acad. Sci. USA **78:**6043–6047.
55. **Morey, C., P. Navarro, E. Debrand, P. Avner, C. Rougeulle, and P. Clerc.** 2004. The region 3′ to Xist mediates X chromosome counting and H3 Lys-4 dimethylation within the Xist gene. EMBO J. **23:**594–604.
56. **Mostoslavsky, R., N. Singh, T. Tenzen, M. Goldmit, C. Gabay, S. Elizur, P. Qi, B. E. Reubinoff, A. Chess, H. Cedar, and Y. Bergman.** 2001. Asynchronous replication and allelic exclusion in the immune system. Nature **414:** 221–225.
57. **Norio, P., S. Kosiyatrakul, Q. Yang, Z. Guan, N. M. Brown, S. Thomas, R. Riblet, and C. L. Schildkraut.** 2005. Progressive activation of DNA replication initiation in large domains of the immunoglobulin heavy chain locus during B cell development. Mol. Cell **20:**575–587.
58. **Ogawa, Y., and J. T. Lee.** 2003. Xite, X-inactivation intergenic transcription elements that regulate the probability of choice. Mol. Cell **11:**731–743.
59. **Paixao, S., I. N. Colaluca, M. Cubells, F. A. Peverali, A. Destro, S. Giadrossi, M. Giacca, A. Falaschi, S. Riva, and G. Biamonti.** 2004. Modular structure of the human lamin B2 replicator. Mol. Cell. Biol. **24:**2958–2967.
60. **Penny, G. D., G. F. Kay, S. A. Sheardown, S. Rastan, and N. Brockdorff.** 1996. Requirement for Xist in X chromosome inactivation. Nature **379:**131–137.
61. **Plenge, R. M., B. D. Hendrich, C. Schwartz, J. F. Arena, A. Naumova, C. Sapienza, R. M. Winter, and H. F. Willard.** 1997. A promoter mutation in the XIST gene in two unrelated families with skewed X-chromosome inactivation. Nat. Genet. **17:**353–356.
62. **Sado, T., Z. Wang, H. Sasaki, and E. Li.** 2001. Regulation of imprinted X-chromosome inactivation in mice by Tsix. Development **128:**1275–1286.
63. **Saha, S., Y. Shan, L. D. Mesner, and J. L. Hamlin.** 2004. The promoter of the Chinese hamster ovary dihydrofolate reductase gene regulates the activity of the local origin and helps define its boundaries. Genes Dev. **18:**397–410.
64. **Simon, I., T. Tenzen, B. E. Reubinoff, D. Hillman, J. R. McCarrey, and H. Cedar.** 1999. Asynchronous replication of imprinted genes is established in the gametes and maintained during development. Nature **401:**929–932.
65. **Singh, N., F. A. Ebrahimi, A. A. Gimelbrant, A. W. Ensminger, M. R. Tackett, P. Qi, J. Gribnau, and A. Chess.** 2003. Coordination of the random asynchronous replication of autosomal loci. Nat. Genet. **33:**339–341.
66. **Staib, C., and F. Grummt.** 1997. Mapping replication origins by nascent DNA strand length. Methods **13:**293–300.
67. **Stavropoulos, N., R. K. Rowntree, and J. T. Lee.** 2005. Identification of developmentally specific enhancers for *Tsix* in the regulation of X chromosome inactivation. Mol. Cell. Biol. **25:**2757–2769.
68. **Takagi, N., O. Sugawara, and M. Sasaki.** 1982. Regional and temporal changes in the pattern of X-chromosome replication during the early postimplantation development of the female mouse. Chromosoma **85:**275–286.
69. **Toledo, F., B. Baron, M. A. Fernandez, A. M. Lachages, V. Mayau, G. Buttin, and M. Debatisse.** 1998. oriGNAI3: a narrow zone of preferential replication initiation in mammalian cells identified by 2D gel and competitive PCR replicon mapping techniques. Nucleic Acids Res. **26:**2313–2321.
70. **Torchia, B. S., and B. R. Migeon.** 1995. The XIST locus replicates late on the active X, and earlier on the inactive X based on FISH DNA replication analysis of somatic cell hybrids. Somat. Cell Mol. Genet. **21:**327–333.
71. **Vassilev, L., and E. M. Johnson.** 1989. Mapping initiation sites of DNA replication in vivo using polymerase chain reaction amplification of nascent strand segments. Nucleic Acids Res. **17:**7693–7705.
72. **Vaughn, J. P., P. A. Dijkwel, and J. L. Hamlin.** 1990. Replication initiates in a broad zone in the amplified CHO dihydrofolate reductase domain. Cell **61:**1075–1087.
73. **Zhang, Z., M. K. Hayashi, O. Merkel, B. Stillman, and R. M. Xu.** 2002. Structure and function of the BAH-containing domain of Orc1p in epigenetic silencing. EMBO J. **21:**4600–4611.
74. **Zhang, Z., K. Shibahara, and B. Stillman.** 2000. PCNA connects DNA replication to epigenetic inheritance in yeast. Nature **408:**221–225.